START PAGE

Chapter 8

INDUCTION MOTORS FOR DRIVES

The induction motor is considered to be the workhorse of industry. It is an AC motor, either three-phase or (for low powers) single phase. Industrial (conventional) induction motors are supplied from constant voltage and frequency industrial power grids for rather constant speed operation. For variable speed drives induction motors are fed from PECs at variable voltage amplitude and frequency.

Like the DC motor, an induction motor consists of a stator (the fixed part) and a rotor (the moving part) mounted on mechanical bearings and separated from the stator by an airgap.

8.1. THE STATOR AND ITS TRAVELING FIELD

The stator consists essentially of a magnetic core made up of punchings (laminations) — 0.1 mm to 0.5mm thick — carrying slot-embedded coils. These coils are interconnected in a certain fashion to constitute the so-called AC armature (primary) winding (Figure 8.1).

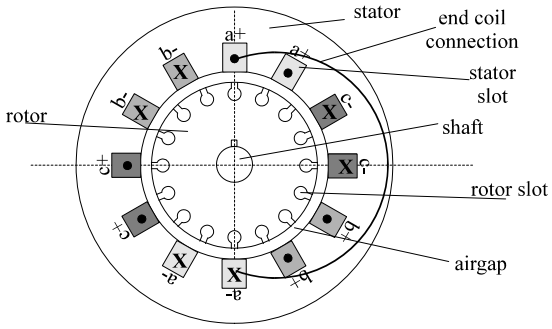

Figure 8.1. Cross section of an induction motor with two poles

The three-phase windings may be placed in slots in a single layer (Figure 8.1) or in two layers. All the coils are, in general, identical and the span is close or equal to what is called the pole pitch τ or the half-period of m.m.f. of that coil or phase. The number of poles per periphery is denoted as 2p.

Under each pole there are three zones, one for each phase. Each phase zone per pole contains q slots (q = 2–8, integer in general). The consecutive phase zones of the same polarity, a_+a_+, b_+b_+ in Figure 8.1. are spatially shifted by a geometrical angle of $2\pi/3p$ which corresponds to 2/3 of pole pitch of the winding.

As one pole pitch corresponds to a semiperiod (180° electrical degrees), the electrical angle α_e is related to the mechanical angle α_g by

$$\alpha_e = p \cdot \alpha_g \tag{8.1}$$

The m.m.f. of each phase coil has a stepwise waveform (Figure 8.2) which is assimilated by a sinusoidal distribution with the semiperiod τ (pole pitch). There are also harmonics which, in general, produce parasitic torques augmented by the rotor and stator slot openings.

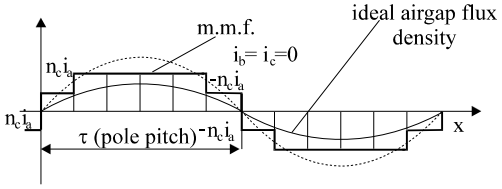

Figure 8.2. The m.m.f. and airgap flux density of phase a.

The phase current is sinusoidal and thus the phase m.m.f. fundamental $F_{a1}(x, t)$ may be written as:

$$F_{a1}(x,t) = F_{a1m} \cdot \sin\frac{\pi}{\tau}x \cdot \sin\omega_1 t \tag{8.2}$$

$$i_a(t) = I\sqrt{2}\sin\omega_1 t \tag{8.3}$$

As the other two phases b, c are space shifted by an electrical angle of $2\pi/3$ and their currents i_b, i_c (in time) by $2\pi/3$, the m.m.f. of phase b and c are

$$F_{b1}(x,t) = F_{a1m} \cdot \sin\left(\frac{\pi}{\tau}x - \frac{2\pi}{3}\right) \cdot \sin\left(\omega_1 t - \frac{2\pi}{3}\right) \tag{8.4}$$

$$F_{c1}(x,t) = F_{a1m} \cdot \sin\left(\frac{\pi}{\tau}x + \frac{2\pi}{3}\right) \cdot \sin\left(\omega_1 t + \frac{2\pi}{3}\right) \tag{8.5}$$

The resultant stator m.m.f. fundamental $F_{s1}(x,t)$ is the sum of F_{a1}, F_{b1} and F_{c1}

$$F_{s1}(x,t) = \frac{3}{2}F_{a1m} \cdot \cos\left(\frac{\pi}{\tau}x - \omega_1 t\right) \tag{8.6}$$

This is evidently a wave traveling along the rotor periphery with the linear speed U_s obtained from

$$\frac{\pi}{\tau}x - \omega_1 t = \text{const.} \tag{8.7}$$

Its increment should be zero

$$\frac{\pi}{\tau}dx - \omega_1 dt = 0$$

Finally

$$U_s = \frac{dx}{dt} = \tau \cdot \frac{\omega_1}{\pi} = 2\tau f_1 \tag{8.8}$$

where f_1 - the primary frequency.

As the airgap is uniform, neglecting the slot openings, the airgap flux density (for zero rotor currents) $B_{g1}(x,t)$ is

$$B_{g1}(x,t) \approx \mu_0 \cdot \frac{F_{s1}(x,t)}{g_e} \tag{8.9}$$

where g_e is an equivalent airgap accounting globally for the slot openings and stator and rotor core magnetic saturation.

Consequently, the three-phase stator winding produces — for zero rotor current — a traveling field in the airgap, with the linear speed $U_s = 2\tau f_1$. As the peripheral speed is related to the angular speed n_1 and the stator bore D_i by

$$U_s = \pi \cdot D_i \cdot n_1 = 2p \cdot \tau \cdot n_1 \tag{8.10}$$

the angular speed of the traveling field n_1 is

$$n_1 = f_1 / p \tag{8.11}$$

n_1 is also called the synchronous speed since for this speed of the rotor no voltages are induced in the rotor windings.

8.2. THE CAGE AND WOUND ROTORS ARE EQUIVALENT

The rotor consists of a laminated core with uniform slotting accommodating either aluminum (copper) bars short-circuited by end-rings (the squirrel cage), Figure 8.3.a., or a three-phase winding (as in the stator) connected to some copper rings and fixed brushes, the wound rotor (Figure 8.3.b).

It has been demonstrated that a symmetric cage (with round bars) may be modeled by an equivalent three-phase winding, that is, a wound rotor.

A PEC or variable resistor may be connected to the wound rotor brushes.

8.3. SLOT SHAPING DEPENDS ON APPLICATION AND POWER LEVEL

Stator slots are either semiclosed (Figure 8.4a) for low and medium power (hundreds of kW) or open (Figure 8.4b) above hundreds of kW when

preformed coils are introduced in slots. Rotor slots for wound rotors are in general semiclosed if the stator ones are open to allow for a rather small airgap (below 2mm) even for high powers (MW and above). Cage rotor slot shapes depend on the power speed level and starting torque requirements in constant frequency fed (industrial) applications.

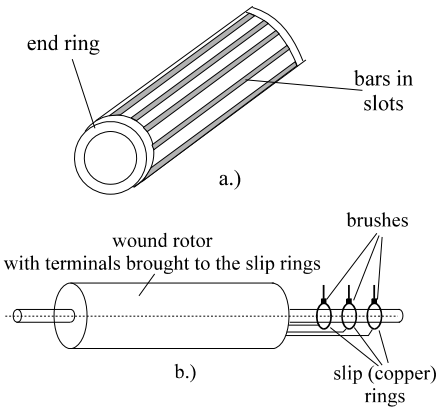

Figure 8.3. Induction motor rotors: a.) cage-type rotor; b.) wound rotor

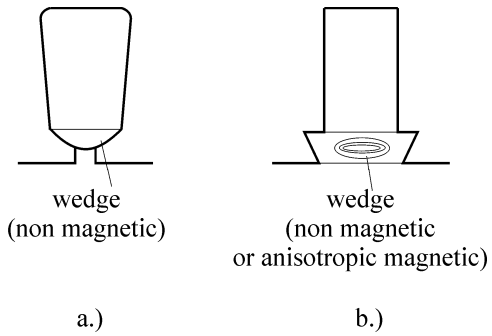

Figure 8.4. Stator or wound rotor slots

a.) for low power (semiclosed slots), b.) for high power (open slots)

Round semiclosed slots (Figure 8.5a.) do not exhibit notable skin effect at start and may be used for constant frequency fed low power low starting torque motors or for variable speed when skin effect is to be avoided.

Skin effect is the concentration of current in the rotor bar towards the upper part of the rotor bar at high rotor frequency (beginning with constant frequency f_1, at standstill when the rotor frequency $f_2 = f_1$). The consequence is an apparent increase in rotor resistance and a less important slot leakage inductance reduction.

Double cages are used in the medium power range to reduce the starting current and increase the starting torque (Figure 8.5e, f). Skin effect (deep

bar) or double cages imply higher rotor resistance and losses at rated speed and thus are to be avoided in variable speed drives. In variable speed (frequency) drives, slots as in Figure 8.5g are proposed to reduce the rotor surface losses.

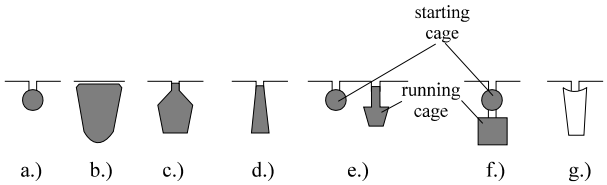

Figure 8.5. Rotor slots:

a.) semiclosed - round for low power and variable frequency motors,

b.) closed - for low noise or high speed motors,

c.) semiclosed with moderate skin effect and starting torque - constant frequency,

d.) semiclosed with high skin effect for high starting torque - constant frequency,

e,f.) double cage - for superhigh starting torque - constant frequency,

g.) for high speed inverter-fed motors.

We entered this discussion as many existing motors are now provided with PECs and thus care must be exercised about performance. Moreover, for constant frequency (speed) operation, the efficient motor category has been introduced — though at lower starting torque and higher starting current. These efficient motors have a short pay-back period due to power loss reduction and are also more adequate in PEC fed variable speed drives.

8.4. THE INDUCTANCE MATRIX

An electric machine is a system of electric and magnetic circuits that are coupled magnetically and electrically. It may be viewed as an assembly of resistances, self-inductances and mutual inductances. We now briefly discuss these inductances.

As a symmetrical rotor cage is equivalent to a three-phase winding we will consider the wound rotor induction motor case (Figure 8.6).

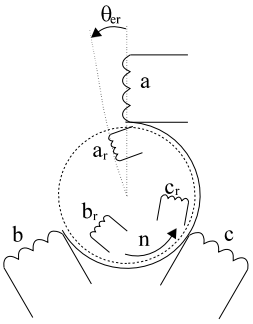

Figure 8.6. Three-phase induction motor with equivalent wound rotor

There are six circuits (phases) and each has a self-inductance and mutual inductances. Let us notice that the self-inductance of phases a, b, c, a_r, b_r, c_r do not depend on rotor position (slot openings are neglected). They have a main part L_{ms}, L_{mr} which corresponds to the flux paths that cross the airgap and embrace all windings on the stator and rotor, and leakage parts L_{ls} and L_{lr} which correspond to the flux paths in the slots, coil end connections, mostly in air, which do not embrace rotor and stator windings.

Let us notice that the airgap flux density of each phase m.m.f is basically sinusoidal along the rotor periphery, and any coupling inductance between phases varies cosinusoidally with the electrical angle of the two windings. Also, mutual inductances on the stator L_{ab}, L_{bc}, L_{ac} and, respectively, on the rotor $L_{a_rb_r}$, $L_{a_rc_r}$, $L_{b_rc_r}$, though referring mainly to flux paths through the airgap, do not depend on rotor position

$$L_{ab} = L_{bc} = L_{ca} = L_{ms}\cos\frac{2\pi}{3} = -\frac{L_{ms}}{2} \tag{8.12}$$

$$L_{a_rb_r} = L_{b_rc_r} = L_{c_ra_r} = L_{mr}\cos\frac{2\pi}{3} = -\frac{L_{mr}}{2} \tag{8.13}$$

Finally, the stator-rotor coupling inductance L_{sr} depends on rotor position through $\cos\theta_{er}$ as the airgap flux density in the airgap produced by any stator phase is sinusoidal

$$L_{sr}(\theta_{er}) = L_{ms}\cdot\frac{W_{re}}{W_{se}}\cos\theta_{er} \tag{8.14}$$

W_{re}, W_{se} are the equivalent turns ratio in the rotor and stator phases

$$\frac{W_{re}}{W_{se}} = \sqrt{\frac{L^r_{mr}}{L_{ms}}} = K_{rs} \tag{8.15}$$

as self-inductances depend on the number of turns squared.

Consequently, $L_{sr}(\theta_{er})$ is

$$L_{sr}(\theta_{er}) = L_{srm}\cos\theta_{er} \tag{8.16}$$

$$L_{srm} = \sqrt{L_{ms}\cdot L^{r}_{mr}} \tag{8.17}$$

The inductances may be now assembled into the so-called matrix inductance $\left[L_{a,b,c,a_r^r,b_r^r,c_r^r}(\theta_{er})\right]$

$$\left[L_{a,b,c,a_r^r,b_r^r,c_r^r}(\theta_{er})\right]=\begin{bmatrix} & a & b & c & a_r & b_r & c_r \\ a & L_{aa} & L_{ab} & L_{ac} & L_{a_ra} & L_{b_ra} & L_{c_ra} \\ b & L_{ab} & L_{bb} & L_{bc} & L_{a_rb} & L_{b_rb} & L_{c_rb} \\ c & L_{ac} & L_{bc} & L_{cc} & L_{a_rc} & L_{b_rc} & L_{c_rc} \\ a_r & L_{a_ra} & L_{a_rb} & L_{a_rc} & L_{a_ra_r} & L_{a_rb_r} & L_{a_rc_r} \\ b_r & L_{b_ra} & L_{b_rb} & L_{b_rc} & L_{a_rb_r} & L_{b_rb_r} & L_{b_rc_r} \\ c_r & L_{c_ra} & L_{c_rb} & L_{c_rc} & L_{a_rc_r} & L_{b_rc_r} & L_{c_rc_r} \end{bmatrix} \tag{8.18}$$

where

$$L_{aa} = L_{bb} = L_{cc} = L_{ls} + L_{ms};\qquad L_{ab} = -L_{ms}/2;\ L_{ac} = -L_{ms}/2;$$

$$L_{a_ra} = L_{b_rb} = L_{c_rc} = L_{srm}\cos\theta_{er};\qquad L_{a_ra_r} = L_{b_rb_r} = L_{c_rc_r} = L^{r}_{lr} + L^{r}_{mr};$$

$$L_{c_ra} = L_{a_rb} = L_{b_rc} = L_{srm}\cos(\theta_{er} - 2\pi/3);$$

$$L_{c_rb} = L_{a_rc} = L_{b_ra} = L_{srm}\cos(\theta_{er} + 2\pi/3);$$

$$L_{a_rb_r} = -L^{r}_{mr}/2;\qquad L_{b_rc_r} = -L^{r}_{mr}/2.$$

8.5. REDUCING THE ROTOR TO STATOR

It is useful to replace the actual rotor winding by an equivalent one with the same performance (and losses) but having the same number of turns per phase as in the stator.

Evidently, for this case, the maximum mutual inductance becomes equal to $L_{ms} = L_{mr}$

$$L_{srm} = L_{ms} \tag{8.19}$$

Denoting the currents and voltages in the rotor with i^{r}_{ar}, i^{r}_{br}, i^{r}_{cr}, V^{r}_{ar}, V^{r}_{br}, V^{r}_{cr} and the ones reduced to the stator as i_{ar}, i_{br}, i_{cr}, V_{ar}, V_{br}, V_{cr}

$$\frac{i_{ar}}{i^{r}_{ar}} = \frac{i_{br}}{i^{r}_{br}} = \frac{i_{cr}}{i^{r}_{cr}} = K_{rs} \tag{8.20}$$

To conserve the rotor input power

$$\frac{V_{ar}}{V_{ar}^{r}} = \frac{V_{br}}{V_{br}^{r}} = \frac{V_{cr}}{V_{cr}^{r}} = \frac{1}{K_{rs}} \tag{8.21}$$

For equal winding losses and leakage magnetic energy

$$\frac{r_r}{r_r^r} = \frac{L_{lr}}{L_{lr}^r} = \frac{1}{K_{rs}^2} \tag{8.22}$$

So the new inductance matrix $\left[L_{a,b,c,a_r,b_r,c_r}(\theta_{er})\right]$ is similar to that in (8.18), but with $L^r{}_{mr} \to L_{ms}, L_{srm} \to L_{ms}$.

Note: For a cage-rotor the expression of the rotor to stator reduction factor K_{rs} of (8.15) is more complicated but, as we do not have access to the cage current, dealing directly with the reduced parameters is common practice. For cage motors, K_{rs} is thus required only for motor design purposes.

We may now pursue the mathematical model in phase coordinates (variables).

8.6. THE PHASE COORDINATE MODEL GOES TO 8th ORDER

In matrix form, with rotor reduced to the stator, the voltage current equations — in stator coordinates for the stator and in rotor coordinates for the rotor — are

$$[V] = [r]\cdot[i] + \frac{d}{dt}[\lambda] \tag{8.23}$$

$$[\lambda] = \left[L_{a,b,c,a_r,b_r,c_r}(\theta_{er})\right]\cdot[i] \tag{8.24}$$

$$[r] = \mathrm{Diag}[r_s, r_s, r_s, r_r, r_r, r_r] \tag{8.25}$$

$$[V] = [V_a, V_b, V_c, V_{ar}, V_{br}, V_{cr}]^T \tag{8.26}$$

$$[i] = [i_a, i_b, i_c, i_{ar}, i_{br}, i_{cr}]^T \tag{8.27}$$

Using (8.24) in (8.23) — with θ_{er} variable in time in any case — we obtain

$$[V] = [r]\cdot[i] + [L]\frac{d[i]}{dt} + \frac{d[L]}{d\theta_{er}}\cdot[i]\cdot\frac{d\theta_{er}}{dt} \tag{8.28}$$

where

$$\frac{d\theta_{er}}{dt} = \omega_r = p\Omega_r \tag{8.29}$$

Ω_r is the mechanical angular speed ($\Omega_r = 2\pi n$).

In the absence of magnetic saturation multiplying (8.28) by $[i]^T$, yields

$$[i]^T \cdot [V] = [i]^T \cdot [r] \cdot [i] + \frac{d}{dt}\frac{1}{2}\left[[L]\cdot[i]\cdot[i]^T\right] + \frac{1}{2}\cdot[i]^T \cdot \frac{d[L]}{d\theta_{er}} \cdot [i] \cdot \omega_r \tag{8.30}$$

The first right term represents the winding losses, the second, the stored energy variation, and the third, the electromagnetic power P_e

$$P_e = T_e \cdot \Omega_r = \frac{1}{2}[i]^T \cdot \frac{d[L]}{d\theta_{er}}[i] \cdot \omega_r \tag{8.31}$$

Finally, the electromagnetic torque T_e is

$$T_e = \frac{1}{2} p \cdot [i]^T \cdot \frac{d[L]}{d\theta_{er}}[i] \tag{8.32}$$

The motion equations are

$$\frac{J}{p}\frac{d\omega_r}{dt} = T_e - T_{load};\ \frac{d\theta_{er}}{dt} = \omega_r \tag{8.33}$$

An 8^{th} order nonlinear model with time variable coefficients (inductances) has been obtained, while still neglecting the core losses. Only numerical methods provide a solution to it. This complex model is to be used directly only in special cases, when the computation effort is justified. Not so for electric drives, in general.

Complex (space-phasor) variables are introduced to obtain a model with position (time) independent coefficients.

8.7. THE SPACE-PHASOR MODEL

Let us introduce first the following notations [1-4]

$$a = e^{j\frac{2\pi}{3}};\ \cos\frac{2\pi}{3} = \mathrm{Re}[a];\ \cos\frac{4\pi}{3} = \mathrm{Re}[a^2];$$

$$\cos\left(\theta_{er} + \frac{2\pi}{3}\right) = \mathrm{Re}\left[a \cdot e^{j\theta_{er}}\right];\ \cos\left(\theta_{er} + \frac{4\pi}{3}\right) = \mathrm{Re}\left[a^2 \cdot e^{j\theta_{er}}\right]; \tag{8.34}$$

Using (8.34) in the flux expression (8.24), the phase a and a_r flux linkages λ_a and λ_{ar} write

$$\lambda_a = L_{ls} \cdot i_a + L_{ms} \cdot \mathrm{Re}\left[i_a + a \cdot i_b + a^2 \cdot i_c\right] + L_{ms} \cdot \mathrm{Re}\left[\left(i_{ar} + a \cdot i_{br} + a^2 \cdot i_{cr}\right) e^{j\theta_{er}}\right] \tag{8.35}$$

$$\lambda_{ar} = L_{lr} \cdot i_{ar} + L_{ms} \cdot \mathrm{Re}\left[i_{ar} + a \cdot i_{br} + a^2 \cdot i_{cr}\right] + L_{ms} \cdot \mathrm{Re}\left[\left(i_a + a \cdot i_b + a^2 \cdot i_c\right) e^{-j\theta_{er}}\right] \tag{8.36}$$

We now introduce the following complex variables as space-phasors

$$\bar{i}_s^{\,s} = \frac{2}{3}\cdot\left(i_a + a\cdot i_b + a^2\cdot i_c\right) \tag{8.37}$$

$$\bar{i}_r^{\,r} = \frac{2}{3}\cdot\left(i_{ar} + a\cdot i_{br} + a^2\cdot i_{cr}\right) \tag{8.38}$$

where

$$\mathrm{Re}\left[\bar{i}_s^{\,s}\right] = i_a - \frac{1}{3}\cdot\left(i_a + i_b + i_c\right) = i_a - i_0 \tag{8.39}$$

$$\mathrm{Re}\left[\bar{i}_r^{\,r}\right] = i_{ar} - \frac{1}{3}\cdot\left(i_{ar} + i_{br} + i_{cr}\right) = i_{ar} - i_0 \tag{8.40}$$

In symmetric transient and steady-state regimes and symmetric windings

$$i_a + i_b + i_c = 0;\ i_{ar} + i_{br} + i_{cr} = 0 \tag{8.41}$$

With definitions (8.37)-(8.38), Equations (8.35)-(8.36) become

$$\lambda_a = L_{ls}\cdot\mathrm{Re}\left(\bar{i}_s^{\,s}\right) + L_m\cdot\mathrm{Re}\left(\bar{i}_s^{\,s} + \bar{i}_r^{\,s}\cdot e^{j\theta_{er}}\right);\ L_m = \frac{3}{2}L_{ms} \tag{8.42}$$

$$\lambda_{ar}^{r} = L_{lr}\cdot\mathrm{Re}\left(\bar{i}_r^{\,s}\right) + L_m\cdot\mathrm{Re}\left(\bar{i}_r^{\,r} + \bar{i}_s^{\,s}\cdot e^{-j\theta_{er}}\right) \tag{8.43}$$

If to (8.42)-(8.43) we add similar equations for phases b, b_r and c, c_r, (8.23) becomes

$$\bar{V}_s^{\,s} = r_s\cdot\bar{i}_s^{\,s} + \frac{d\bar{\lambda}_s^{\,s}}{dt} = r_s\cdot\bar{i}_s^{\,s} + L_s\cdot\frac{d\bar{i}_s^{\,s}}{dt} + L_m\frac{d\left(\bar{i}_r^{\,r}e^{j\theta_{er}}\right)}{dt} \tag{8.44}$$

$$\bar{V}_r^{\,r} = r_r\cdot\bar{i}_r^{\,r} + \frac{d\bar{\lambda}_r^{\,r}}{dt} = r_r\cdot\bar{i}_r^{\,r} + L_r\cdot\frac{d\bar{i}_r^{\,r}}{dt} + L_m\frac{d\left(\bar{i}_s^{\,s}e^{-j\theta_{er}}\right)}{dt} \tag{8.45}$$

with

$$L_s = L_{ls} + L_m;\ \ L_r = L_{lr} + L_m \tag{8.46}$$

and

$$\bar{V}_s^{\,s} = \frac{2}{3}\cdot\left(V_a + a\cdot V_b + a^2\cdot V_c\right);\quad \bar{V}_r^{\,r} = \frac{2}{3}\cdot\left(V_{ar} + a\cdot V_{br} + a^2\cdot V_{cr}\right) \tag{8.47}$$

The complex variables $\bar{V}_s^{\,s}, \bar{V}_r^{\,r}, \bar{i}_s^{\,s}, \bar{i}_r^{\,r}, \bar{\lambda}_s^{\,s}, \bar{\lambda}_r^{\,r},$ are still represented in their respective coordinates (stator for stator, rotor for rotor). We may now use a rotation of the complex variables by the angle θ_b in the stator and by θ_b–θ_{er} in the rotor to obtain a unique coordinate system at some speed ω_b

$$\omega_b = \frac{d\theta_b}{dt} \tag{8.48}$$

$$\bar{\lambda}_s^{\,s} = \bar{\lambda}_s^{\,b} \cdot e^{j\theta_b};\ \bar{i}_s^{\,s} = \bar{i}_s^{\,b} \cdot e^{j\theta_b};\ \bar{V}_s^{\,s} = \bar{V}_s^{\,b} \cdot e^{j\theta_b} \tag{8.49}$$

$$\bar{\lambda}_r^{\,r} = \bar{\lambda}_r^{\,b} \cdot e^{j(\theta_b-\theta_{er})};\ \bar{i}_r^{\,r} = \bar{i}_r^{\,b} \cdot e^{j(\theta_b-\theta_{er})};\ \bar{V}_r^{\,r} = \bar{V}_r^{\,b} \cdot e^{j(\theta_b-\theta_{er})} \tag{8.50}$$

With the new variables, (8.44)-(8.45) become

$$\begin{aligned} \bar{V}_s &= r_s \cdot \bar{i}_s + \frac{d\bar{\lambda}_s}{dt} + j \cdot \omega_b \cdot \bar{\lambda}_s \\ \bar{V}_r &= r_r \cdot \bar{i}_r + \frac{d\bar{\lambda}_r}{dt} + j \cdot (\omega_b - \omega_r) \cdot \bar{\lambda}_r \end{aligned} \tag{8.51}$$

with

$$\bar{\lambda}_s = L_s \cdot \bar{i}_s + L_m \cdot \bar{i}_r \tag{8.52}$$

$$\bar{\lambda}_r = L_r \cdot \bar{i}_r + L_m \cdot \bar{i}_s \tag{8.53}$$

Notice that for clarity we dropped the superscript b.

The torque should be calculated from (8.32) with the above notations

$$T_e = \frac{3}{2} \cdot p \cdot \mathrm{Re}\left(j \cdot \bar{\lambda}_s \cdot \bar{i}_s^{\,*}\right) = -\frac{3}{2} \cdot p \cdot \mathrm{Re}\left(j \cdot \bar{\lambda}_r \cdot \bar{i}_r^{\,*}\right) \tag{8.54}$$

Equations (8.51)-(8.54) together with the equations of motion (8.33) constitute the complex variable or space-phasor model of the induction machine with single rotor cage and with core loss neglected.

We may now decompose in plane the space-phasors along two orthogonal axes d and q moving at speed ω_b [5]

$$\begin{aligned} &\bar{V}_s = V_d + j \cdot V_q;\ \ \bar{i}_s = i_d + j \cdot i_q;\ \ \bar{\lambda}_s = \lambda_d + j \cdot \lambda_q \\ &\bar{V}_r = V_{dr} + j \cdot V_{qr};\ \ \bar{i}_r = i_{dr} + j \cdot i_{qr};\ \ \bar{\lambda}_r = \lambda_{dr} + j \cdot \lambda_{qr} \end{aligned} \tag{8.55}$$

With (8.55) the two voltage equations (8.51) become

$$
\begin{aligned}
V_d &= r_s \cdot i_d + \frac{d\lambda_d}{dt} - \omega_b \cdot \lambda_q \\
V_q &= r_s \cdot i_q + \frac{d\lambda_q}{dt} + \omega_b \cdot \lambda_d \\
V_{dr} &= r_r \cdot i_{dr} + \frac{d\lambda_{dr}}{dt} - (\omega_b - \omega_r) \cdot \lambda_{qr} \\
V_{qr} &= r_r \cdot i_{qr} + \frac{d\lambda_{qr}}{dt} + (\omega_b - \omega_r) \cdot \lambda_{dr} \\
T_e &= \frac{3}{2} p(\lambda_d i_q - \lambda_q i_d) = \frac{3}{2} p L_m (i_q i_{dr} - i_d i_{qr})
\end{aligned}
\tag{8.56}
$$

Also from (8.49)-(8.50) and (8.47)

$$
\begin{bmatrix} V_d \\ V_q \\ V_0 \end{bmatrix} = [P(\theta_b)] \cdot \begin{bmatrix} V_a \\ V_b \\ V_c \end{bmatrix}
\tag{8.57}
$$

$[P(\theta_b)]$ is the Park transformation

$$
[P(\theta_b)] = \frac{2}{3} \cdot \begin{bmatrix} \cos(-\theta_b) & \cos\left(-\theta_b + \frac{2\pi}{3}\right) & \cos\left(-\theta_b - \frac{2\pi}{3}\right) \\ \sin(-\theta_b) & \sin\left(-\theta_b + \frac{2\pi}{3}\right) & \sin\left(-\theta_b - \frac{2\pi}{3}\right) \\ \frac{1}{2} & \frac{1}{2} & \frac{1}{2} \end{bmatrix}
\tag{8.58}
$$

The inverse of Park transformation is

$$
[P(\theta_b)]^{-1} = [P(\theta_b)]^T
\tag{8.59}
$$

A similar transformation is valid for rotor quantities with $\theta_b - \theta_{er}$ replacing θ_b in (8.58).

It may be proved that the homopolar components V_0, i_0, V_{0r}, i_{0r} have separate equations and do not interfere in the energy conversion process in the motor.

$$
\begin{aligned}
\bar{V}_0 &= r_s \cdot \bar{i}_0 + \frac{d\bar{\lambda}_{0s}}{dt}; \quad \bar{\lambda}_0 \approx L_{ls} \cdot \bar{i}_0 \\
\bar{V}_{0r} &= r_r \cdot \bar{i}_{0r} + \frac{d\bar{\lambda}_{0r}}{dt}; \quad \bar{\lambda}_{0r} \approx L_{lr} \cdot \bar{i}_{0r}
\end{aligned}
\tag{8.60}
$$

Equations (8.56)-(8.60) represent the dq0 model of the induction machine that operates with real (not complex) variables. The complex variable (space-phasor) and d-q model are equivalent as they are based on

identical assumptions (symmetric sinusoidally distributed windings and constant airgap). The speed of the reference system ω_b is arbitrary as the airgap is uniform.

Up to now we rushed through equations to quickly obtain the complex variable (d-q) model of the induction machine; we now insist on some graphical representations to facilitate the assimilation of this new knowledge.

Example 8.1. The space-phasor of sinusoidal symmetric currents

Consider three symmetrical sinusoidal currents and show how their complex space-phasor $\bar{i}_s^{\,s}$ varies in time through 6 instants. Give a graphical description of this process in time.

Solution:

The three-phase currents may be written as

$$i_{a,b,c} = I\sqrt{2}\cdot\cos\left(\omega_1 t-(i-1)\cdot\frac{2\pi}{3}\right);\ i=1,2,3 \tag{8.61}$$

The space-phasor in stator coordinates $\overline{i_s^{\,s}}$ is (8.37)

$$\bar{i}_s^{\,s}=\frac{2}{3}I\sqrt{2}\left[\cos\omega_1 t+e^{j\frac{2\pi}{3}}\cos\left(\omega_1 t-\frac{2\pi}{3}\right)+e^{j\frac{4\pi}{3}}\cos\left(\omega_1 t-\frac{4\pi}{3}\right)\right] \tag{8.62}$$

with
$$e^{j\frac{2\pi}{3}}=\cos\frac{2\pi}{3}+j\cdot\sin\frac{2\pi}{3};\ e^{j\frac{4\pi}{3}}=\cos\frac{4\pi}{3}+j\cdot\sin\frac{4\pi}{3} \tag{8.63}$$

(8.62) becomes
$$\bar{i}_s^{\,s}=I\sqrt{2}\left[\cos\omega_1 t+j\cdot\sin\omega_1 t\right]=i_d+j\cdot i_q \tag{8.64}$$

The position of the space-phasor for $\omega_1 t=0,\frac{\pi}{3},\frac{2\pi}{3},\pi,\frac{4\pi}{3},\frac{5\pi}{3}$ is shown in Figure 8.7.

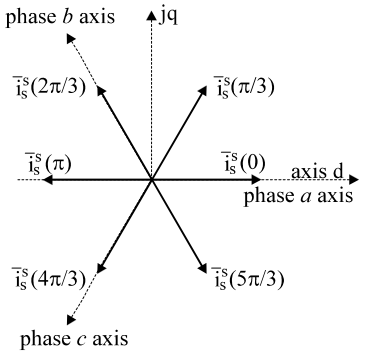

Figure 8.7. The space-phasor of sinusoidal three-phase currents

It should be noticed that the time "produces" the instantaneous values of currents while the definition of the space-phasor shows that each phase current instantaneous value is placed along the axis of the corresponding phase. So, in fact, the space-phasor travels in the d-q stator plane with the electrical angular speed equal to ω_1.

The same concept is applied to flux linkages and thus their space-phasor is related to the traveling field in AC machines.

Also note that

$$\mathrm{Re}\left[\bar{i}_s^{\,s}\right] = i_a; \quad \text{if } i_a + i_b + i_c = 0 \tag{8.65}$$

8.8. THE SPACE-PHASOR DIAGRAM FOR ELECTRICAL TRANSIENTS

The space-phasor model equations (8.51)-(8.53) may be represented on a space-phasor diagram in the d-q plane, with axes d and q rotating at speed $\omega_b = \omega_1$ (Figure 8.8). Let us consider $\bar{V}_r^{\,b} = 0$.

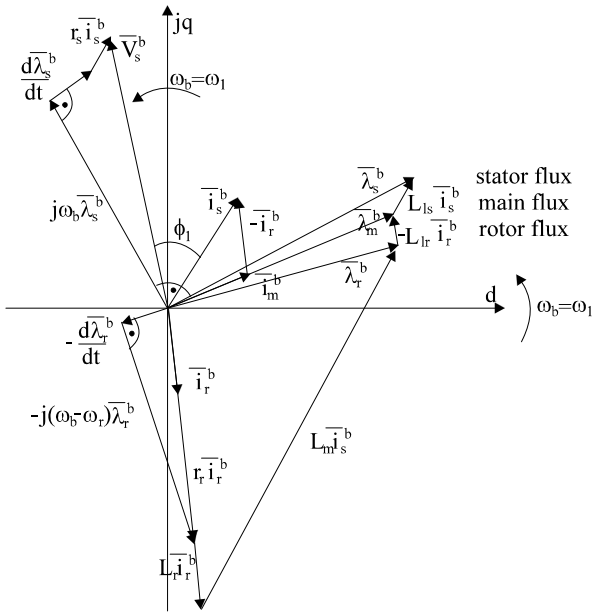

Figure 8.8. The space-phasor diagram of induction motor valid for transients (for steady d/dt = 0) in synchronous coordinates (cage rotor: $\bar{V}_r^{\,b} = 0$).

As ω_1 is the frequency of the actual stator voltages at steady-state, for this latter case d/dt = 0. In general, during steady-state

$$d/dt = j(\omega_1 - \omega_b). \tag{8.66}$$

Also for steady-state the rotor flux equation (8.52) becomes

$$\begin{aligned}\overline{V}_r{}^b &= r_r \cdot \bar{i}_r{}^b + j(\omega_1 - \omega_b)\cdot \overline{\lambda}_r{}^b + j(\omega_b - \omega_r)\cdot \overline{\lambda}_r{}^b = \\ &= r_r \cdot \bar{i}_r{}^b + j(\omega_1 - \omega_r)\cdot \overline{\lambda}_r{}^b\end{aligned} \tag{8.67}$$

Only for $\overline{V}_r{}^b = 0$ (short-circuited, cage, rotor) the rotor current and flux space-phasors are *orthogonal to each other*.

For this case the torque expression (8.54) becomes

$$T_e = \frac{3}{2} p \cdot \lambda_r{}^b \cdot i_r{}^b; \quad \left|\overline{\lambda}_r{}^b\right| = \text{ct.} \tag{8.68}$$

8.9. ELECTRICAL TRANSIENTS WITH FLUX LINKAGES AS VARIABLES

Equations (8.52)-(8.53) at constant speed allow for the elimination of rotor and stator currents $\bar{i}_s{}^b$ and $\bar{i}_r{}^b$.

With

$$\bar{i}_s{}^b = \sigma^{-1}\left(\frac{\overline{\lambda}_s{}^b}{L_s} - \frac{\overline{\lambda}_r{}^b \cdot L_m}{L_s L_r}\right) \tag{8.69}$$

$$\bar{i}_r{}^b = \sigma^{-1}\left(\frac{\overline{\lambda}_r{}^b}{L_r} - \frac{\overline{\lambda}_s{}^b \cdot L_m}{L_s L_r}\right) \tag{8.70}$$

$$\sigma = 1 - \frac{L_m{}^2}{L_s L_r} \tag{8.71}$$

(8.50)-(8.51) become

$$\tau_s' \frac{d\overline{\lambda}_s{}^b}{dt} + (1 + j \cdot \omega_b \cdot \tau_s')\cdot \overline{\lambda}_s{}^b = \tau_s' \overline{V}_s{}^b + K_r \overline{\lambda}_r{}^b \tag{8.72}$$

$$\tau_r' \frac{d\overline{\lambda}_r{}^b}{dt} + (1 + j \cdot (\omega_b - \omega_r)\cdot \tau_r')\cdot \overline{\lambda}_r{}^b = \tau_r' \overline{V}_r{}^b + K_s \overline{\lambda}_s{}^b \tag{8.73}$$

with

$$\begin{aligned} K_s &= \frac{L_m}{L_s}; \quad K_r = \frac{L_m}{L_r} \\ \tau_s' &= \tau_s \cdot \sigma; \quad \tau_r' = \tau_r \cdot \sigma \\ \tau_s &= \frac{L_s}{r_s}; \quad \tau_r = \frac{L_r}{r_r} \end{aligned} \tag{8.74}$$

While τ_s, τ_r are the stator and rotor time constants, τ_s' and τ_r' are transient time constants of the stator and rotor.

The structural diagram corresponding to (8.72)-(8.73) is shown on Figure 8.9.

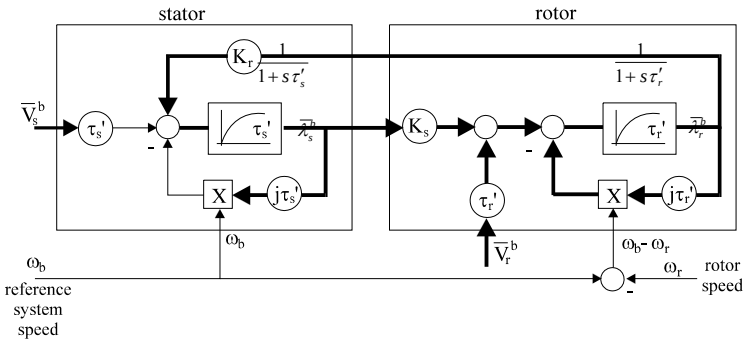

Figure 8.9. Structural diagram of induction motor with stator and rotor flux $\bar{\lambda}_s^b$ and $\bar{\lambda}_r^b$ as variables; random speed (ω_b) coordinates.

8.10. COMPLEX EIGENVALUES FOR ELECTRICAL TRANSIENTS

Equations (8.72)-(8.73) imply a second-order complex variable system with only two complex eigenvalues corresponding to the determinant

$$\begin{vmatrix} \tau_s'\underline{s}+1+j\omega_b\tau_s' & -K_r \\ -K_s & \tau_r'\underline{s}+1+j(\omega_b-\omega_r)\tau_r' \end{vmatrix} = 0 \tag{8.75}$$

The complex eigenvalues $\underline{s}_{1,2}$ from (8.75) depend on the reference system speed ω_b and on rotor speed ω_r, but their real part is, in general, negative suggesting attenuated periodic response [4,6].

Example 8.2. For an induction motor with the data $r_s = 0.5\Omega$, $r_r = 0.60\Omega$, $L_s = L_r = 0.08$H, $L_m = 0.075$H, p = 2 pole pairs, calculate the complex eigenvalues for constant speed, in synchronous coordinates ($\omega_1 = 2\pi 60$) for n = 0 and n = 1800 rpm.

Solution:

The value of $\omega_b = \omega_1 = 2\pi 60$ rad/s. σ, τ_s', τ_r', K_s, K_r are now calculated from (8.71)-(8.74)

$$\sigma = 1 - \frac{L_m^{\,2}}{L_s L_r} = 1 - \frac{0.075^2}{0.08^2} = 0.1211 \tag{8.76}$$

$$\tau_s' = \sigma\tau_s = \sigma\frac{L_s}{r_s} = 0.1211 \cdot \frac{0.08}{0.5} = 0.01937\,\text{s} \tag{8.77}$$

$$\tau_r' = \sigma\tau_r = \sigma\frac{L_r}{r_r} = 0.1211\cdot\frac{0.08}{0.6} = 0.01614\,\text{s} \tag{8.78}$$

$$K_s = \frac{L_m}{L_s} = \frac{0.075}{0.08} = 0.9375 \tag{8.79}$$

$$K_r = \frac{L_m}{L_r} = \frac{0.075}{0.08} = 0.9375 \tag{8.80}$$

Also
$$\omega_r = 2\pi pn = 4\pi n \tag{8.81}$$

Now we rewrite (8.75) in a canonical form

$$\begin{gathered}\underline{s}^2\tau_s'\tau_r' + \underline{s}\left[\left(\tau_s' + \tau_r'\right) + j\tau_s'\tau_r'\left(2\omega_b - \omega_r\right)\right] \\ + \left(1 + j\cdot\omega_b\cdot\tau_s'\right)\left(1 + j\cdot\left(\omega_b - \omega_r\right)\cdot\tau_r'\right) - K_sK_r = \\ \underline{s}^2\cdot 0.01937\cdot 0.01614 + \\ \underline{s}\left[\left(0.01937 + 0.01614\right) + j\cdot 0.01937\cdot 0.01614\cdot\left(2\cdot 376.8 - 4\pi n\right)\right] \\ + \left(1 + j\cdot 376.8\cdot 0.01937\right)\cdot\left(1 + j\cdot\left(376.8 - 4\pi n\right)\cdot 0.01614\right) \\ - 0.9375^2 = 0\end{gathered} \tag{8.82}$$

It is evident that the roots s depend on speed n. The solving of the second order equation is straightforward.

8.11 ELECTRICAL TRANSIENTS FOR CONSTANT ROTOR FLUX

By constant rotor flux we mean, in general, constant amplitude at ($\omega_1 - \omega_b$) frequency. For synchronous coordinates it would mean zero frequency.

So constant rotor flux means that in (8.72)-(8.73)

$$\frac{d\bar{\lambda}_r^{\,b}}{dt} = j\cdot\left(\omega_1 - \omega_b\right)\cdot\bar{\lambda}_r^{\,b} \tag{8.83}$$

Using (8.83) in (8.73)

$$\bar{\lambda}_r^{\,b} = \frac{\tau_r'\bar{V}_r^{\,b} + K_s\bar{\lambda}_s^{\,b}}{1 + jS\omega_1\tau_r'} \tag{8.84}$$

It is more convenient to use synchronous coordinates for equations (8.72):

$$\tau_s'\frac{d\bar{\lambda}_s^{\,b}}{dt} + \left(1 + j\cdot\omega_1\cdot\tau_s'\right)\cdot\bar{\lambda}_s^{\,b} = \tau_s'\bar{V}_s^{\,b} + K_r\bar{\lambda}_r^{\,b} \tag{8.85}$$

Equations (8.84)-(8.85) lead to a simplification in the structural diagram of figure 8.9 as the derivative term in the rotor disappears (Figure 8.10).

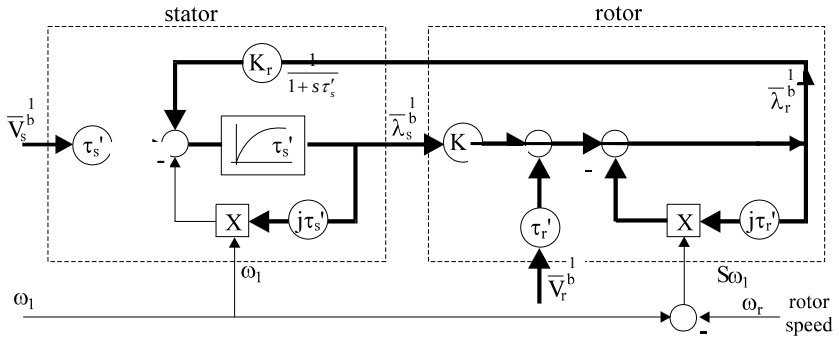

Figure 8.10. Structural diagram of induction motor with constant rotor flux and speed in synchronous coordinates ($\omega_b = \omega_1$)

The system's order is reduced and thus the stator flux presents only one complex eigenvalue as may be inferred from (8.84)-(8.85).

8.12. STEADY-STATE: IT IS DC IN SYNCHRONOUS COORDINATES

Steady-state means, in general, that the three-phase voltages are symmetric and sinusoidal:

$$V_{a,b,c} = V\sqrt{2}\cdot\cos\left(\omega_1 t - (i-1)\cdot\frac{2\pi}{3}\right);\ i = 1, 2, 3 \tag{8.86}$$

The voltage space-phasor in random coordinates is

$$\overline{V}_s^{\,b} = \frac{2}{3}\left[V_a(t) + V_b(t)\cdot e^{j\frac{2\pi}{3}} + V_c(t)\cdot e^{-j\frac{2\pi}{3}}\right]\cdot e^{-j\theta_b} \tag{8.87}$$

with (8.86)

$$\overline{V}_s^{\,b} = V\sqrt{2}\left[\cos(\omega_1 t - \theta_b) + j\cdot\sin(\omega_1 t - \theta_b)\right] \tag{8.88}$$

For steady-state

$$\theta_b = \omega_b t + \theta_0 \tag{8.89}$$

Consequently

$$\overline{V}_s^{\,b} = V\sqrt{2}\left[\cos\left[(\omega_1 - \omega_b)t - \theta_0\right] + j\cdot\sin\left[(\omega_1 - \omega_b)t - \theta_0\right]\right] =$$
$$= \quad V\sqrt{2}\cdot e^{j\left[(\omega_1-\omega_b)t-\theta_0\right]} \tag{8.90}$$

It is obvious that, for steady-state, the currents in the model must have the voltage frequency, which is: $(\omega_1 - \omega_b)$. Once again for steady-state we use (8.51), with d/dt = $j\cdot(\omega_1 - \omega_b)$ as inferred in (8.66).

Consequently from (8.51)

$$\begin{aligned}\overline{V}_{s0}{}^{b} &= r_s\cdot\bar{i}_{s0}{}^{b} + j\cdot\omega_1\cdot\overline{\lambda}_{s0}{}^{b}\\ \overline{V}_{r0}{}^{b} &= r_r\cdot\bar{i}_{r0}{}^{b} + j\cdot S\omega_1\cdot\overline{\lambda}_{r0}{}^{b};\ \ S = 1-\omega_r/\omega_1\end{aligned} \tag{8.91}$$

S is known as slip.

So the form of steady-state equations is independent of the reference speed ω_b. What counts is the primary (stator) frequency ω_1 and the actual rotor currents frequency $S\omega_1$.

Notice that, for synchronous coordinates, steady-state means $d/dt = j(\omega_1-\omega_b) = 0$, that is *DC quantities*.

In the flux equations (8.52)-(8.53) we may separate the main (airgap) flux linkage $\overline{\lambda_m}$

$$\overline{\lambda}_s{}^{b} = L_{ls}\cdot\bar{i}_s{}^{b} + \overline{\lambda}_m;\ \ \overline{\lambda}_m = L_m\cdot\left(\bar{i}_s{}^{b} + \bar{i}_r{}^{b}\right) = L_m\cdot\bar{i}_m{}^{b} \tag{8.92}$$

$$\overline{\lambda}_r{}^{b} = L_{lr}\cdot\bar{i}_r{}^{b} + \overline{\lambda}_m \tag{8.93}$$

Equations (8.91)-(8.93) lead to the standard equivalent circuit of Figure 8.11.

Magnetic saturation may be considered through $\lambda_m(i_m)$ functions approximating measurements or field distribution calculations. [7]

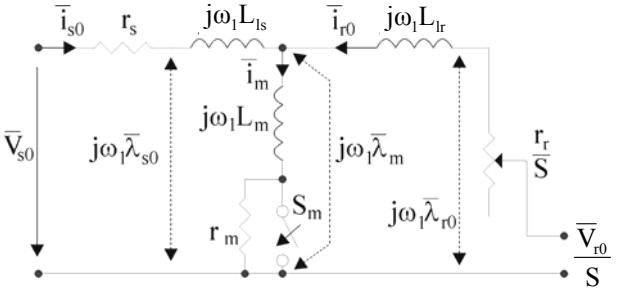

Figure 8.11. Space-phasor steady-state equivalent circuit of induction machine

Note (on core loss): The core loss occurs mainly in the stator as $\omega_1 >> S\omega_1$; that is, the frequency of magnetic fields is higher in the stator since the rated slip is S_n = 0.08-0.005 (decreasing with power). An equivalent resistance r_m — determined from experiments — may be included in the equivalent circuit, Figure 8.11, to account for the core losses during steady-

state. For investigating the role of core loss during transients, additional stator windings in the d-q model have to be included (see [7]).

The torque expression (8.54) and $V_{r0}^{b} = 0$, yields

$$T_e = -\frac{3}{2} p \cdot \mathrm{Re}\left(j\bar{\lambda}_r^{b} \cdot \bar{i}_r^{b*}\right) \tag{8.94}$$

From (8.91)

$$\bar{i}_{r0} = -j \cdot S\omega_1 \cdot \frac{\bar{\lambda}_{r0}}{r_r} \tag{8.95}$$

Consequently the electromagnetic torque T_e is

$$T_e = \frac{3}{2} p \cdot \frac{\lambda_{r0}^{\ 2}}{r_r} \cdot S\omega_1 \tag{8.96}$$

Using the equivalent circuit of Figure (8.11) and (8.95) we may obtain the conventional torque expression

$$T_e = \frac{3p}{\omega_1} \frac{V^2 \cdot r_r / S}{\left(r_s + c_1 r_r / S\right)^2 + \omega_1^{\ 2}\left(L_{ls} + c_1 L_{lr}\right)^2} \tag{8.97}$$

with

$$c_1 \approx 1 + \frac{L_{ls}}{L_m} \tag{8.98}$$

8.13. NO-LOAD IDEAL SPEED MAY GO UNDER OR OVER CONVENTIONAL VALUE ω_1

The no-load ideal speed (slip S_0) corresponds to zero torque, that is, (8.91), zero rotor current

$$\overline{V_{r0}^{\ b}} = j \cdot S_0 \omega_1 \cdot \overline{\lambda_{r0}^{\ b}} \tag{8.99}$$

Only for short-circuited rotor windings (or passive impedance at rotor terminals) ($\overline{V_r^{\ b}} = 0$), the ideal no-load slip $S_0 = 0$ and $\omega_{ro} = \omega_1$.

When the induction machine is doubly fed ($\overline{V}_r^{\ b} \neq 0$), the ideal no-load slip is different from zero and the no-load ideal speed is, in general

$$\omega_{r0} = \omega_1\left(1 - S_0\right) \tag{8.100}$$

The value and phase shift between $\overline{V}_{r0}^{\ b}$ and $\bar{\lambda}_{r0}^{\ b}$ could be arranged through a PEC supplying the wound rotor. So S_0 could be either positive or negative. Thus only for $\overline{V}_r^{\ b} \neq 0$ from (8.96) the torque is positive (motoring), for S>0 and negative (generating) for S<0.

The doubly fed induction motor could operate either as a motor or as a generator below and above $\omega_{r0} = \omega_1$ ($S_0 = 0$), provided that the PEC can produce bidirectional power flow between the wound rotor and the power grid. These doubly fed induction motor drives will be dealt with separately in Chapter 14 dedicated to high power industrial drives.

Example 8.3. For steady-state, calculate the stator voltage, stator flux, current, power factor, torque of an induction motor at 10% ideal no-load (synchronous) speed ω_1 and S = 0.02.

The motor data are $r_s = 0.5\Omega$, $r_r = 0.6\Omega$, $L_s = L_r = 0.08$H, $L_m = 0.075$H, $\lambda_{r0} = 0.8$Wb, $\omega_1 = 2\pi 60$ rad/s, p = 2 pole pairs, $V_r^b = 0$ (cage rotor).

Solution:

First we have to calculate the initial conditions, which are implicitly steady-state. Let us use synchronous coordinates

$$\omega_{r0} = \omega_1(1 - S) \tag{8.101}$$

So:
$$(\omega_1)_{t=0} = \frac{\omega_{r0}}{1 - (S)_{t=0}} = \frac{0.1 \cdot 2 \cdot \pi \cdot 60}{1 - 0.02} = 38.45 \quad \text{rad/s} \tag{8.102}$$

The torque (T_e) is (8.96)

$$(T_e)_{t=0} = \frac{3}{2} p \cdot (\lambda_r^b)^2 \cdot \frac{S\omega_1}{r_r} = \frac{3}{2} \cdot 2 \cdot (0.8)^2 \cdot 0.02 \cdot \frac{2\pi 60}{0.6} = 24.115 \quad \text{Nm} \tag{8.103}$$

From (8.73) with d/dt = 0 and $V_r^b = 0$, we may now calculate the stator flux $\bar{\lambda}_s^b$

$$\bar{\lambda}_s^b = \bar{\lambda}_r^b \cdot \frac{1 + j \cdot S \cdot \omega_1 \cdot \tau_r'}{K_s} \tag{8.104}$$

Note that the motor parameters are as in example 8.2 and thus $\tau_r' = 0.01614$s, $\tau_s' = 0.01937$s, $K_s = K_r = 0.9375$, $\sigma = 0.1211$.

$$\bar{\lambda}_s^b = \bar{\lambda}_r^b \cdot \frac{1 + j \cdot 0.02 \cdot 2\pi 60 \cdot 0.01614}{0.9375} = 0.8533 + j0.1038 \tag{8.105}$$

Let us consider the d axis along the rotor flux and thus $\bar{\lambda}_r^b = \lambda_r^b$.

Now from (8.72) with $\frac{d\bar{\lambda}_s^b}{dt} = 0$ we may find the stator voltage $\bar{V}_s^b$

$$\bar{V}_s{}^b = \frac{(1 + j\omega_1\tau_s')\bar{\lambda}_s{}^b - K_r \cdot \bar{\lambda}_r{}^b}{\tau_s'} =$$

$$= \frac{(1 + j \cdot 2\pi 60 \cdot 0.01937) \cdot 0.8 \cdot (1.066 + j0.1297) - 0.9375 \cdot 0.8}{0.01937}$$

$$= -33.74 + j326.69; \quad V_s{}^b = 328.4\text{V} \tag{8.106}$$

The motor phase voltage (r.m.s. value)

$$V = V_s{}^b / \sqrt{2} = 328.4 / 1.41 = 232.91 \text{ V} \tag{8.107}$$

The stator current is obtained from (8.69)

$$\bar{i}_s{}^b = \frac{\left[\bar{\lambda}_s{}^b - \bar{\lambda}_r{}^b \cdot K_r\right]}{\sigma \cdot L_s} =$$

$$\frac{\left[0.8 \cdot (1.066 + j0.1297) - 0.8 \cdot 0.9357\right]}{0.1211 \cdot 0.08} = 10.76 + j10.71 \tag{8.108}$$

The rotor space-phasor $\bar{i}_r{}^b$ is (8.95)

$$\bar{i}_r{}^b = -jS\omega_1 \frac{\lambda_r{}^b}{r_r} = -j \cdot 0.02 \cdot 2\pi 60 \cdot \frac{0.8}{0.6} = -j10.05 \text{ A} \tag{8.109}$$

The amplitude of the stator current $i_s{}^b = 15.181$ A. The results are illustrated by the space-phasor diagram in Figure 8.12.

The power factor angle φ_1 is

$$\varphi_1 = \arg \bar{V}_s{}^b - \arg \bar{i}_s{}^b = \frac{\pi}{2} + \tan^{-1} \frac{33.74}{326.69} - \tan^{-1} \frac{10.71}{10.76} =$$

$$= 90° + 5.9° - 45.156° = 50.74° \tag{8. 110}$$

Finally, $\cos\varphi_1 = 0.633$.

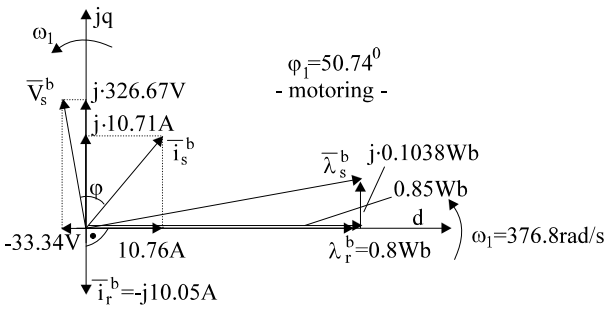

Figure 8.12. Steady-state space-phasor diagram in synchronous coordinates ($\omega_b = \omega_1$):

DC quantities

Example 8.4. Loss breakdown

A high efficiency induction motor with cage rotor has the data rated power $P_n = 5kW$, rated line voltage (rms) $V_L = 220V$ (star connection), rated frequency $f_1 = 60Hz$, number of pole pairs $p = 2$, core loss (P_{iron}) = mechanical loss $P_{mec} = 1.5\%$ of P_n, additional losses $p_{add} = 1\%P_n$, stator per rotor winding losses $p_{cor}/p_{cos} = 2/3$, rated efficiency $\eta_n = 0.9$ and power factor $\cos\varphi_n = 0.88$.

Calculate all loss components, phase current (rms), then rated slip, speed, electromagnetic torque, shaft torque and stator current (as space-phasors).

Solution:

The loss breakdown diagram of the induction motor is shown in Figure 8.13.

The input power P_{in} is

$$P_{in} = \frac{P_{out}}{\eta_n} = \frac{5000}{0.9} = 5555.55 \text{ W} \tag{8.111}$$

The phase current I_n (rms) is

$$I_n = \frac{P_{in}}{\sqrt{3} \cdot V_L \cdot \cos\varphi_n} = \frac{5555.55}{\sqrt{3} \cdot 220 \cdot 0.88} = 16.58 \text{ A} \tag{8.112}$$

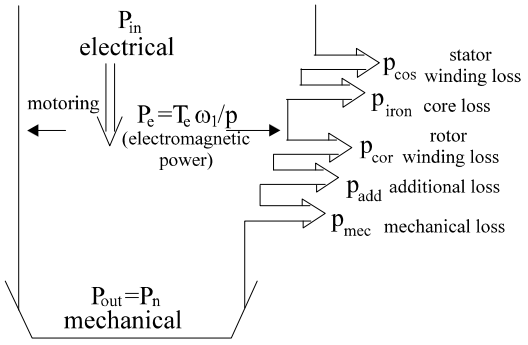

Figure 8.13. Induction motor energy conversion

The total losses $\sum p$ are

$$\sum p = P_{in} - P_{out} = 5555.55 - 5000 = 555.55 \text{ W} \tag{8.113}$$

Consequently

$$p_{iron} = p_{mec} = 0.015 \cdot 5000 = 75\text{W} \tag{8.114}$$

$$p_{add} = 0.01 \cdot 5000 \ \text{W} \tag{8.115}$$

So

$$p_{cos} + p_{cor} = \sum p - p_{iron} - p_{mec} - p_{add} = 555.55 - 75 - 75 - 50 \approx 355\text{W} \tag{8.116}$$

$$p_{cos} + \frac{2}{3} p_{cos} = 355\text{W} \tag{8.117}$$

$$p_{cos} = 213.3\ \text{W};\ p_{cor} = 142\ \text{W} \tag{8.118}$$

The electromagnetic power P_e is the active power that crosses the airgap

$$P_e = P_{in} - P_{cos} - p_{iron} = T_e \cdot \frac{\omega_1}{p} \tag{8.119}$$

$$P_e = 5555.55 - 213 - 75 = 5267\ \text{W} \tag{8.120}$$

$$T_e = \frac{5267}{2\pi 60} \cdot 2 = 27.956\ \text{Nm} \tag{8.121}$$

The rotor winding loss p_{cor} is

$$p_{cor} = S_n \cdot P_e \tag{8.122}$$

and thus the rated slip is

$$S_n = \frac{142}{5267} = 0.02696 \tag{8.123}$$

The rated speed n_n is

$$n_n = \frac{f_1}{p}(1 - S_n) = \frac{60}{2}(1 - 0.02696) = 29.1912\text{rps} = 1751.472\text{rpm} \tag{8.124}$$

The shaft torque T_n is calculated directly from mechanical power P_n

$$T_n = \frac{P_n}{2\pi n_n} = \frac{5000}{2\pi \cdot 29.1912} = 27.274\text{Nm} < T_e \tag{8.125}$$

Finally the amplitude of the stator current, $\bar{i}_s$ in synchronous coordinates (DC quantities) is

$$i_s = i_n \sqrt{2} = 16.58 \cdot 1.41 = 23.3778\ \text{A} \tag{8.126}$$

Note: To calculate all motor parameters, resistances and inductances, more data are required. This is beyond our scope in this example, however.

8.14. MOTORING, GENERATING, AC BRAKING

The equivalent circuit for steady-state (Figure 8.11) shows that the active power in the rotor (the electromagnetic power P_e), is

$$P_e = 3 \cdot I_{r0}{}^2 \cdot \frac{r_r}{S} = T_e \cdot \frac{\omega_1}{p}; \quad S = 1 - \frac{\omega_r}{\omega_1} \tag{8.127}$$

This expression is valid for the cage rotor ($V_r{}^b = 0$).

Motoring mode is defined as the situation when the torque has the same sign as the speed

$$P_e > 0, T_e > 0; \quad \omega_r > 0 \Rightarrow 0 < S < 1 \tag{8.128}$$

For *generating* the torque is negative (S<0) in (8.127) but the speed is positive

$$P_e < 0, T_e < 0; \quad \omega_r > 0 \Rightarrow S < 0 \tag{8.129}$$

The generator produces braking ($T_e < 0$, $\omega_r > 0$) but the energy transfer direction in the motor is reversed. The energy is pumped back into the power source through the stator.

Braking is obtained when again ($T_e > 0$, $\omega_r < 0$) (or $T_e < 0$, $\omega_r > 0$) but the electromagnetic power is still positive

$$\begin{aligned} &P_e > 0; T_e > 0; \omega_r < 0 \Rightarrow S > 1 \\ &P_e > 0; T_e < 0; \omega_r > 0 \Rightarrow S > 1 \end{aligned} \tag{8.130}$$

We may synthesize the results on operation modes as in Table 8.1.

Table 8.1. Operation modes (cage rotor)

S	-∞ - - - - - - - 0 + + + + + + 1 + + + + + + + +∞		
ω_r	+∞ + + + + + + ω_1 + + + + + + 0 - - - - - - - - - -∞		
T_e	0 - - - - - - - - 0 + + + + + + T_e(start) + + + + + 0		
P_e	- - - - - - - - - 0 + + + + + + + + + + + + + + +		
mode	**Generating**	**Motoring**	**AC braking**

Using the torque expression (8.97) we may find the maximum torque for the critical slip:

$$S_k = \frac{\pm c_1 r_r}{\sqrt{r_s{}^2 + \omega_1{}^2 \left(L_{ls} + c_1 L_{lr}\right)^2}}; c_1 = 1 + \frac{L_{sl}}{L_m} \tag{8.131}$$

$$T_{ek} = \frac{3p}{\omega_1} \cdot \frac{V^2}{2c_1\left(r_s \pm \sqrt{r_s^{\,2} + \omega_1^{\,2}\left(L_{ls} + c_1 L_{lr}\right)^2}\right)} \tag{8.132}$$

The torque slip (speed) curve is shown in Figure 8.14.

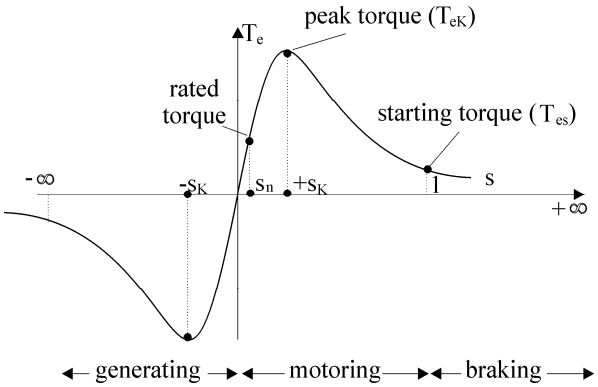

Figure 8.14. Torque/speed curve of induction motors for constant voltage and frequency

Using the definition of critical slip S_k and torque T_{ek} in the torque expression (8.97) we obtain, after some approximations, the Kloss formula

$$\frac{T_e}{T_{ek}} \approx \frac{2}{\frac{S}{S_k} + \frac{S_k}{S}} \tag{8.133}$$

8.15. DC BRAKING: ZERO BRAKING TORQUE AT ZERO SPEED

For moderate braking requirements DC braking is commonly used in modern electrical drives. To calculate the DC braking torque we redraw the space-phasor equivalent circuit in Figure 8.11 but with a DC stator current source space-phasor in Figure 8.15.

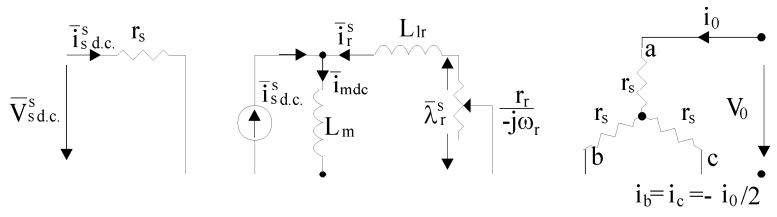

Figure 8.15. Equivalent circuit for DC braking - stator coordinates - in space-phasors; steady-state.

The electromagnetic torque is still computed from (8.94)

$$T_e = \frac{3}{2} p \lambda_{rdc} i_{rdc} = -\frac{3}{2} p \frac{i_{rdc}^{\ 2} \cdot r_r}{\omega_r} \tag{8.134}$$

with

$$\bar{i}_{rdc}^{\ s} = \bar{i}_{sdc}^{\ s} \cdot \frac{L_m}{L_r - j\frac{r_r}{\omega_r}} \tag{8.135}$$

Finally

$$T_e = -\frac{3}{2} p \frac{L_m^{\ 2} \cdot i_{sdc}^{\ 2} \cdot \omega_r \cdot r_r}{L_r^{\ 2} \omega_r^{\ 2} + r_r^{\ 2}} \tag{8.136}$$

The peak torque is obtained for ω_{rk}

$$\omega_{rk} = \frac{r_r}{L_r} = \frac{1}{\tau_r} \tag{8.137}$$

and its value is

$$T_{ek} = -\frac{3}{2} p \frac{L_m^{\ 2} \cdot i_{sdc}^{\ 2}}{2 L_r} \tag{8.138}$$

The braking torque may be modified through the DC current level in the stator. The PEC can produce the phase connection in Figure 8.15b where the current complex variable in stator coordinates is

$$\bar{i}_{sdc}^{\ s} = \frac{2}{3}\left(i_a + i_b e^{j\frac{2\pi}{3}} + i_c e^{-j\frac{2\pi}{3}}\right) = \frac{2}{3}\left(i_0 - \frac{i_0}{2} 2\cos\frac{2\pi}{3}\right) = i_0 \tag{8.139}$$

The torque speed curve for DC braking is shown in Figure 8.16. Notice also that the rotor kinetic energy is dumped into the rotor resistor and that for zero speed the braking torque is zero. Also, above ω_{rk} (which is fairly small in high efficiency motors), the torque is again rather small.

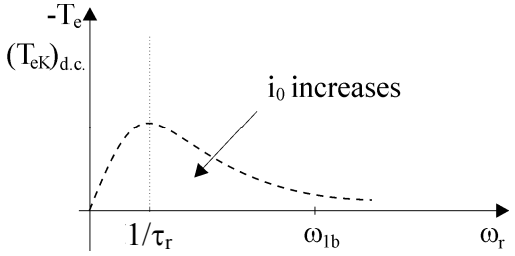

Figure 8.16. DC braking torque of induction motors

8.16. SPEED CONTROL METHODS

Variable speed is required in many applications. It has to be performed at high energy conversion rates.

The no-load ideal speed ω_{r0} is ((8.100) with (8.99))

$$\omega_{r0} = \omega_1\left[1 + \mathrm{Im ag}\left(\frac{\overline{V}_{r0}{}^{b}}{\omega_1 \overline{\lambda}_{r0}{}^{b}}\right)\right];\quad \omega_1 = \omega_r + \omega_2 \tag{8.140}$$

Evidently for the cage rotor $\overline{V}_r{}^{b} = 0$ and thus $\omega_{r0} = \omega_1 = 2\pi f_1$ or

$$n_0 = \frac{\omega_{r0}}{2\pi p} = \frac{f_1}{p} \tag{8.141}$$

ω_2 is the frequency of the rotor current (or of $\overline{V}_{r0}$ through rotor side PEC). There are three essential methods to vary speed by changing the no-load ideal speed (as the rated slip is small) as suggested by (8.140):

- stator frequency f_1 variation;
- pole number (2p) changing;
- *wound rotor supply* (or rotor frequency f_2 variation).

While pole number 2p changing involves either a separate stator winding or a special winding with a switch to change from $2p_1$ to $2p_2$ poles (Dahlander winding) the other two methods require variable frequency either in the stator or in the rotor, obtainable with PECs in the stator and, respectively, in the rotor.

For limited speed variation, the power rating of rotor-side PEC is smaller than that of the PEC in the stator. In high power applications the rotor PEC solution with a wound rotor induction motor is the one preferred for limited speed range (±30%) control.

Stator frequency control is far more frequently used, especially for wide speed control range. However, the level of flux depends on the current in the machine, especially on the magnetization current

$$\bar{I}_m = \bar{I}_s{}^{b} + \bar{I}_r{}^{b} \tag{8.142}$$

Consequently, it is crucial to control I_m properly to avoid excessive magnetic saturation, while varying frequency f_1.

So we have to adopt either voltage V_s and frequency f_1 coordinated control or current $\bar{I}_s$ (or $\bar{I}_m$) and frequency f_1 control. In general V_1/f_1 coordinated change is applied. There is an infinity of possibilities to relate $\overline{V}_s(V_1)$ or $\bar{I}_s(\bar{I}_m)$ to frequency f_1 to obtain the desired performance. However, only three main methods reached the markets:

- V_1/f_1 - scalar control;
- constant (controlled) rotor flux (λ_r) vector control;

- constant (controlled) stator flux (λ_s) - vector control.

Here only the torque/speed curves obtainable with the above methods are given. Notice that in all these cases the PEC voltage supplying the induction motor is voltage limited with the maximum voltage reached at base speed ω_b.

8.17. V_1 / f_1 TORQUE/SPEED CURVES

V_1/f_1 control means that:

$$V_1 = V_0 + K_f \cdot f_1 \tag{8.143}$$

We may judge the torque/speed curves obtained in this case through the critical slip S_k and torque T_{ek} of (8.131)-(8.132). The critical slip increases notably with f_1 (ω_1) reduction while the critical torque is only slightly decreased with f_1 decrease at frequencies above 5Hz. Below this value the peak torque decreases dramatically if (8.143) is applied (Figure 8.17). For a safe start $V = V_0 + K \cdot f_1$ is applied to compensate for the stator resistance drop $r_s i_s$

$$V_0 = c_0 r_s i_{sn} \tag{8.144}$$

V_0 is called the voltage boost and amounts to a few percent of rated voltage V_n, higher for low power motors.

Above rated (base) speed the voltage remains constant and invariably the critical torque decreases and, eventually, constant power is preserved up to a maximum frequency f_{1max}. Above base speed, if we neglect the voltage drop $r_s \bar{i}_s$ in (8.91), the stator equation (for steady-state) is

$$V_{s0} \approx j\omega_1 \bar{\lambda}_{s0}{}^b; \qquad \omega_1 > \omega_b \tag{8.145}$$

So, for constant voltage V_{s0}, the stator flux λ_{s0} and, consequently, the main flux λ_m decrease with speed (frequency) increasing above ω_b. This zone — ω_b to ω_{1max} — is called the flux weakening zone. In many applications constant power is required for a ratio ω_{1max}/ω_b of 2-4. The entire motor design (sizing) depends on this requirement in terms of both electromagnetic and thermal loading.

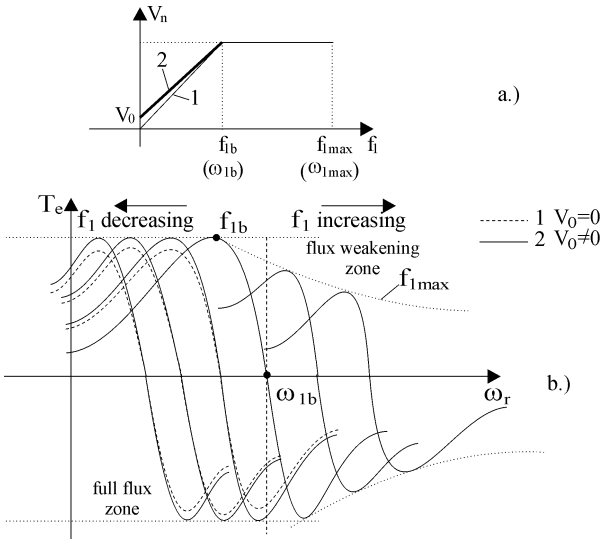

Figure 8.17. Torque/speed curves for $V_1 = V_0 + K_f \cdot f_1$ (V_1/f_1 control):

a.) V_1/f_1 dependences, b.) T_e/ω_r curves;

V_1/f_1 drives are standard with low dynamics applications and moderate speed control range ($\omega_{1b}/\omega_{1min}$ = 10 - 15 or so) such as pumps or fans where the load torque is solely dependent on speed and thus an optimal V_1/f_1 relationship may be calculated off line — for maximum efficiency or power factor — and implemented in the drive hardware.

8.18. ONLY FOR CONSTANT ROTOR FLUX TORQUE/SPEED CURVES ARE LINEAR

The torque expression for constant rotor flux λ_r^b is (8.96)

$$T_e = \frac{3}{2} p \frac{\lambda_{r0}{}^2 (\omega_1 - \omega_r)}{r_r} \tag{8.146}$$

and it represents a straight line (Figure 8.18). This is ideal for speed (or torque) control purposes and led to (now widely accepted in industry), vector control. It is, however, to be noted that above base frequency ω_{1b}, when the full voltage capability of PEC is reached, the value of rotor flux magnitude may not be maintained any more as the difference between the stator flux (8.145) and rotor flux amplitudes (8.104) is less than 15% in general (lower values for higher powers). So, above ω_{1b}, the torque/speed curves degenerate into the shapes obtained for V_1/f_1 control.

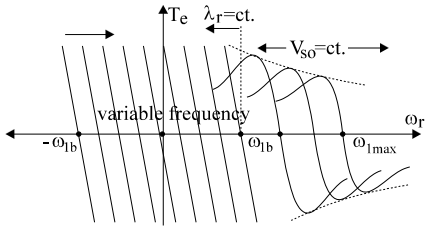

Figure 8.18. Torque/speed curves for constant rotor flux λ_r^b = ct. up to base frequency ω_{1b}; constant voltage and variable frequency above ω_{1b}.

Four-quadrant operation presented in Figure 8.18 is obtainable as with V_1/f_1 control.

Negative frequency ω_1 means negative (reverse) m.m.f. wave speed, to be obtained by changing the stator phase voltage sequence (from a b c to a c b).

8.19. CONSTANT STATOR FLUX TORQUE/SPEED CURVES HAVE TWO BREAKDOWN POINTS

Let us note from (8.104) that the stator-rotor flux relationship for steady-state (cage rotor) is

$$\bar{\lambda}_{s0} = \bar{\lambda}_{r0}\frac{(1 + jS\omega_1\tau_r')}{K_s} \tag{8.147}$$

Consequently the torque T_e from (8.146) becomes

$$T_e = \frac{3}{2}p\frac{K_s^2}{r_r}\frac{S\omega_1\lambda_{s0}^2}{1+(S\omega_1\tau_r')^2} \tag{8.148}$$

This expression has extreme (critical) values for

$$(S\omega_1)_k = \pm\frac{1}{\tau_r'} \tag{8.149}$$

$$T_{ek} = \frac{3}{2}p\frac{K_s^2\lambda_s^2}{2r_r\tau_r'} \tag{8.150}$$

So the peak torque is independent of frequency as long as λ_s amplitude may be realized, that is, below base (rated) frequency.

Above base frequency, according to (8.145), the approximate peak torque would be

$$(T_{ek})_{\omega_1>\omega_{1b}} = \frac{3}{2}p\frac{K_s^2}{2r_r\tau_r'}\cdot\frac{V_{s0}^2}{\omega_1^2} \tag{8.151}$$

The torque/speed curves are shown in Figure 8.19 for four-quadrant operation.

The peak torque is safely provided even for zero speed. Still the departure from linearity in the torque/speed curve has to be dealt with when investigating electric drive transients and stability.

Note: In principle, PECs can also provide constant main (airgap) flux, variable frequency control. So far this operation mode has not reached wide markets in variable speed drives.

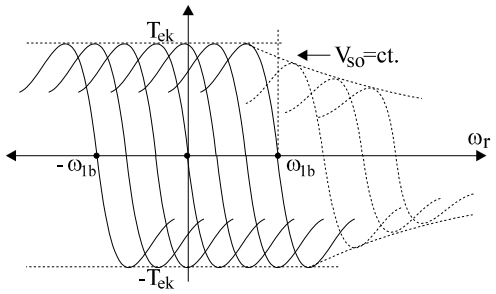

Figure 8.19. Torque/speed curves for constant stator flux amplitude λ_s up to ω_{1b} and constant voltage above ω_{1b}.

8.20. THE SPLIT-PHASE INDUCTION MOTOR

The split-phase induction motor is provided with two orthogonal stator windings: the main winding and the auxiliary winding.

This induction motor is, in general, fed from a single phase AC supply of constant or variable voltage and frequency.

So, even for variable speed, it requires, essentially, a single phase PWM inverter.

Connecting a capacitor in series with the auxiliary winding causes the current I_a to lead the current in the main winding I_m and thus the two orthogonal placed windings produce an elliptical magnetic field in the airgap which has a traveling component. This explains the safe selfstarting from the capacitor auxiliary to the main winding direction of rotation.

Switching the capacitor from auxiliary to main winding leads to the reversal of traveling field component in the airgap and thus the direction of motion may be reversed. For this latter case the two windings should be identical (same number of turns and slots). For unidirectional motion, a higher than unity turns ratio a $=W_a/W_m$ is typical with $I_a < I_m$, as in many cases the auxiliary winding is turned off after starting the motor.

It is also common to use two capacitors: one (larger) for starting, and a smaller one for running.

It goes without saying that the power factor of the capacitor split-phase IM is very good, due to the presence of the capacitor.

Typical connections for dual capacitors IM are shown in Fig. 8.20.

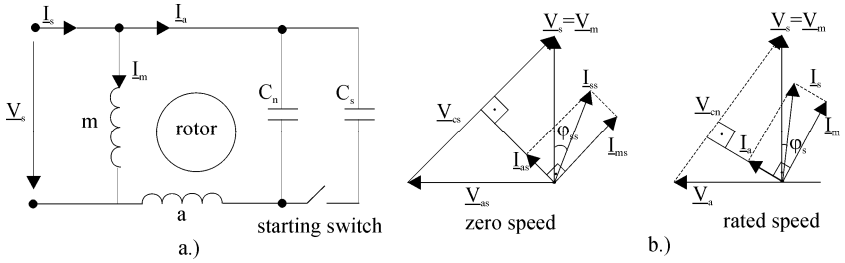

Figure 8.20. The dual capacitor IM: a.) Equivalent scheme,

b.) Phasor diagrams for zero and rated load.

The capacitor voltage is rectangular to auxiliary winding current. For symmetry conditions – 90° electrical degrees between the I_a and I_m and equal Ampere turns $W_mI_m = W_aI_a$ – a pure traveling field is produced; once at zero speed with the capacitor C_s and once at rated speed (load) with capacitor $C_n < C_s$ ($C_s / C_n \cong 4 - 6$).

At any other speed (slip S) the magnetic field in the airgap will have an additional (undesirable) inverse component which produces a braking torque and additional losses.

As done for the three phase motor, the m.m.f. of stator windings fundamental components are:

$$\begin{aligned} F_m(\theta_{es}, t) &= F_{lm}\cos(\omega_1 t)\cos\theta_{es} \\ F_a(\theta_{es}, t) &= -F_{la}\cos(\omega_1 t + \gamma_i)\sin\theta_{es} \end{aligned} \tag{8.152}$$

The ratio of the two m.m.f. amplitudes is:

$$\frac{F_{la}}{F_{lm}} = \frac{W_m k_{Wm1}}{W_a k_{Wa1}} \frac{I_m}{I_a} = \frac{1}{a}\frac{I_m}{I_a} \tag{8.153}$$

The total m.m.f. $F(\theta_{es}, t)$ may be decomposed in forward and backward waves:

$$\begin{aligned} F(\theta_{es}, t) &= F_m(\theta_{es}, t) + F_a(\theta_{es}, t) = \\ F_{lm}\cos(\omega_1 t)\cos\theta_{es} &+ F_{la}\cos(\omega_1 t + \gamma_i)\sin\theta_{es} = \\ \frac{1}{2}F_m C_f \sin(\theta_{es} - \omega_1 t - \beta_f) &+ \frac{1}{2}F_m C_b \sin(\theta_{es} + \omega_1 t - \beta_b) \end{aligned} \tag{8.154}$$

With:

$$C_f = \sqrt{\left(1+\frac{F_{1a}}{F_{1m}}\sin\gamma_i\right)^2 + \left(\frac{F_{1a}}{F_{1m}}\right)^2 \cos^2\gamma_i} \tag{8.155}$$

$$C_b = \sqrt{\left(1-\frac{F_{1a}}{F_{1m}}\sin\gamma_i\right)^2 + \left(\frac{F_{1a}}{F_{1m}}\right)^2 \cos^2\gamma_i} \tag{8.156}$$

$$\sin\beta_f = \frac{1+\frac{F_{1a}}{F_{1m}}\sin\gamma_i}{C_f};\ \ \sin\beta_b = \frac{1-\frac{F_{1a}}{F_{1m}}\sin\gamma_i}{C_b} \tag{8.157}$$

It is evident that for $F_{1a}/F_{1m} \cong 1$ and the phase shift $\gamma_i=90^0$, $C_b=0$ and thus the backward field (and torque) is zero. The slip is $S_+=(\omega_1 - \omega_r) / \omega_1$ for the direct m.m.f. component and $S_- = 2\text{-}S = (-\omega_1 - \omega_r) / (-\omega_1)$ for the backward (inverse) m.m.f. component.

For the steady state the symmetrical (+ / −) component model is straightforward, while for transients the dq model in stator coordinates is very practical.

The + / − model

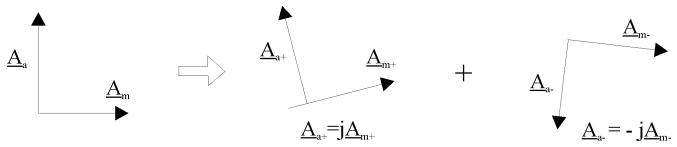

Figure 8.21. The + / − model decomposition;

The superposition principle is used:

$$\underline{A}_m = \underline{A}_{m+} + \underline{A}_{m-};\ \ \underline{A}_a = \underline{A}_{a+} + \underline{A}_{a-} \tag{8.158}$$

And

$$\underline{A}_{m+} = \frac{1}{2}\left(\underline{A}_m - j\underline{A}_a\right);\underline{A}_{m-} = \underline{A}^*_{m+} \tag{8.159}$$

Now the machine behaves like two separate fictitious machines for the two components:

$$\begin{aligned} &\underline{V}_{m+} = \underline{Z}_{m+}\underline{I}_{m+};\underline{V}_{m-} = \underline{Z}_{m-}\underline{I}_{m-} \\ &\underline{V}_{a+} = \underline{Z}_{a+}\underline{I}_{a+};\underline{V}_{a-} = \underline{Z}_{a-}\underline{I}_{a-} \end{aligned} \tag{8.160}$$

$$\underline{V}_m = \underline{V}_{m+} + \underline{V}_{m-};\ \ \underline{V}_a = \underline{V}_{a+} + \underline{V}_{a-} \tag{8.161}$$

The + / − impedances $\underline{Z}_{m\pm}$ represent the total forward/backward impedances of the machine on a per phase basis, when the rotor cage is reduced to the main (m) and respectively, auxiliary (a) winding (Figure 8.22)

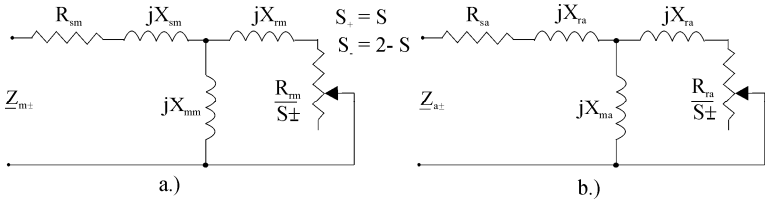

Figure 8.22. Equivalent symmetrical (+ / −) impedance: a.) reduced to main winding; b.) reduced to auxiliary winding;

The relationship of $\underline{V}_m$ and $\underline{V}_a$ voltages to the source voltage $\underline{V}_s$ are:

$$\underline{V}_s = \underline{V}_m ; \underline{V}_a + (\underline{I}_{a+} + \underline{I}_{a-})\underline{Z}_a = \underline{V}_s \tag{8.162}$$

$\underline{Z}_a$ is the auxiliary impedance (a capacitor in general) added in series to the auxiliary phase for better starting and (or) running.

The torque T_e expression has two terms: the feedforward and feedback components:

$$T_e = T_{e+} + T_{e-} = \frac{2p_1}{\omega_1}\left[I_{rm+}^2 \frac{R_{rm}}{S} - I_{rm-}^2 \frac{R_{rm}}{2-S} \right] \tag{8.163}$$

When the auxiliary winding is open $Z_a = \infty$, $I_{rm+} = I_{rm-}$ and thus, at zero speed (S=1) the torque is zero, as expected, and the machine does not start.

A typical mechanical characteristic $T_e(\omega_r)$ for a split phase capacitor run motor comprises the positive torque (with synchronism at $+\omega_1$) and the negative torque (with synchronism at $-\omega_1$), Figure 8.23.

The backward (negative) torque is rather small but present at all speeds, less the rated speed, where, by design, symmetry conditions are met. There are two symmetrization conditions that stem from $I_{m-}=0$ which lead to a value of turns ratio a and of the capacitance C for given slip S [8, pp. 851].

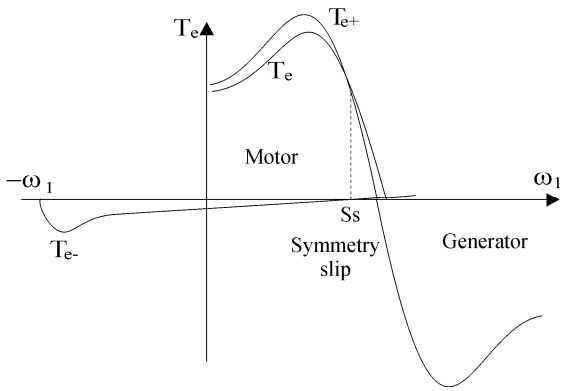

Figure 8.23. Typical mechanical characteristic of a split phase capacitor-run induction motor;

For the case of motor with same copper quantity in both stator windings the symmetrization conditions are very simple [8]:

$$a = X_{m+} / R_{m+} = \tan \varphi_{+}$$
$$X_c = \frac{1}{\omega C} = Z_{+} \cdot a\sqrt{a+1} \tag{8.164}$$

So for an existing motor (with fixed turns ratio a), there may not be any capacitor to symmetrize the motor at no slip (speed). Fortunately perfect symmetrization is not necessary because the backward torque tends to be small for reasonably low rotor resistance (good efficiency) designed motors.The slip phase capacitor motor is widely used both at constant and variable speed for applications below 500W in general. More on the control of this motor in Chapter 9.

Example 8.4:

A capacitor run split-phase IM with $C_a = 8\mu F$, 2p = 6 pole, 230V, 50 Hz, $n_n = 960$ rpm has the following main and auxiliary winding parameters: $R_{sm} = 34\Omega$, $R_{sa} = 150\Omega$, a = 1.73, $X_{sm} = 35.9\Omega$, $X_{sa} = a^2X_{sm}$, $X_{rm} = 29.32\Omega$, $R_{rm} = 23.25\Omega$, $X_m = 249\Omega$.

For the case of open auxiliary phase calculate:

a) The ± impedances $\underline{Z}_{m\pm}$, $\underline{Z}_{m\pm}$ at rated slip;

b) The equivalent circuit of the machine for this particular case;

c) The main winding current components I_{m+}, I_{m-} and the total current I_m.

d) The ± torque components, the resultant torque and the mechanical power, efficiency and power factor.

Solution:

a) The rated slip:

$$S_n = \frac{\omega_1 - \omega_r}{\omega_1} = \frac{2\pi 50 - 2\pi 3 \cdot 960/60}{2\pi 50} = 0.06; 2 - S = 1.94; \tag{8.165}$$

From Figure 8.22. the ± impedances are:

$$\underline{Z}_{m+} = R_{sm} + jX_{sm} + Z_{r+} = 34 + j35.9 + \frac{j249(23.25/0.06 + j29.32)}{23.25/0.06 + j(29.32 + 249)} =$$
$$= 34 + j35.9 + 105.4 + j174 \tag{8.166}$$

$$\underline{Z}_{m-} = R_{sm} + jX_{sm} + Z_{r-} = 34 + j35.9 + \frac{j249(23.25/1.94 + j29.32)}{23.25/1.94 + j(29.32 + 249)} =$$
$$= 34 + j35.9 + 9.6 + j27 \tag{8.167}$$

Let us notice that because the auxiliary current $\underline{I}_a = 0$, from (8.158) – (8.159):

$$\underline{I}_{m+} = \underline{I}_{m-} = \frac{\underline{I}_m}{2}$$

Combining this with (8.160):

$$\underline{V}_m = \underline{V}_s = \underline{V}_{m+} + \underline{V}_{m-} = \underline{Z}_{m+}\underline{I}_{m+} + \underline{Z}_{m-}\underline{I}_{m-} == \underline{I}_m\left(\frac{Z_{m+}}{2} + \frac{Z_{m-}}{2}\right)$$

which means that we obtain a series equivalent circuit (Fig. A):

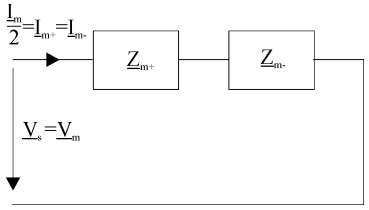

Figure A. Single phase ($\underline{I}_a$=0) IM equivalent circuit;

c) The main winding current components $\underline{I}_{m+}$=$\underline{I}_{m-}$ are then simply:

$$I_{m+} = I_{m-} = \frac{V_s}{\left|\underline{Z}_{m+} + \underline{Z}_{m-}\right|} = \frac{230}{2 \cdot 165.2} = 0.696\text{A}$$

The main winding current $I_m = 2I_{m+} = 1.392$ A.
The power factor for S = 0.06, $\cos\varphi_1$ is:

$$\cos\varphi_1 = \frac{\mathrm{Real}(\underline{Z}_{m+} + \underline{Z}_{m-})}{\left|\underline{Z}_{m+} + \underline{Z}_{m-}\right|} = \frac{2 \cdot 92.8}{2 \cdot 165.2} = 0.5617!$$

d) The torque components in (8.163) are (Fig. A):

$$T_e = T_{e+} + T_{e-} = \frac{2p}{\omega_1}\left[I_{m+}^2 \frac{R_{rm}}{S} - I_{m-}^2 \frac{R_{rm}}{2-S}\right]$$

With R_{rm+}= 105.4 Ω and R_{rm-}= 9.6 Ω from $\underline{Z}_{m+}$ and $\underline{Z}_{m-}$ above:

$$T_{e+} = \frac{2 \cdot 3}{2\pi 50} 0.696^2 \cdot 105.4 = 0.9756\text{Nm}$$

$$T_{e-} = -\frac{2 \cdot 3}{2\pi 50} 0.696^2 \cdot 9.6 = -0.08886\text{Nm}$$

So the total torque:

$$T_e = T_{e+} + T_{e-} = 0.8687\text{Nm}$$

The mechanical power P_m is:

$$P_m = T_e 2\pi 50 = 0.8687 \cdot 2\pi \cdot \frac{940}{60} = 85.47\text{W}$$

Neglecting the core and mechanical loss the efficiency is:

$$\eta = \frac{P_m}{P_m + P_{Co}} = \frac{85.47}{85.47 + 1.392^2 \cdot 34} = 0.5647$$

The power factor $\cos\varphi_1$ is low, as calculated above because the capacitor is missing and the efficiency is low, mainly because the power is small.

The need to supply the auxiliary winding in series with a capacitor is evident.

Note: Even when the auxiliary phase winding is present, the performance computation process is as above, but a bit more tedious [8, pp. 847].

8.21. SUMMARY

- The three-phase induction motor is the workhorse of industry for powers from below 1 kW to 10 MW and over 100 MW in wound rotor configuration for pumped storage power plants.
- The AC stator and rotor windings are placed in slots. Skin effect in the rotor windings is put to work in constant speed high starting torque applications and is to be avoided in variable speed drives where variable voltage and frequency are provided by PECs.

- The inductances, between stator and rotor windings, vary sinusoidally with the rotor position and thus the voltage-current equations in phase coordinates are difficult to handle for transients even through numerical methods, in an 8^{th} order nonlinear system.
- The space-phasor model, equivalent to the d-q (orthogonal axis, or Park's) model, is characterized by constant coefficients.
- For steady-state, the rotor current and flux space-phasors are spatially orthogonal to each other.
- At constant speed the space-phasor model is a second-order system with two complex eigenvalues, one for the stator, the other for the rotor. They depend on rotor speed and on the reference system speed ω_b, but their real part is negative for low slip values.
- Under steady-state the space-phasor model has the same equations irrespective of the reference system speed.
- Losses in an induction motor are distributed both in the stator and in the rotor: winding and core loss in the stator and winding, and additional and mechanical losses in the rotor. The equivalent circuit allows for calculating the steady-state performance conveniently.
- The induction motor operation modes are motoring, generating and AC braking (plugging). The torque/speed curve shows two peak values (one for motoring and the other for generating), where constant voltage and frequency fed.
- When the motor stator is DC current fed and the rotor speed is nonzero, motion induced voltages in the rotor produce rotor currents and as a consequence a braking torque. Its maximum is obtained at a small speed for cage rotor motors, as the rotor current frequency ω_2 is equal to rotor speed ω_r.
- Speed control methods include variable stator or rotor frequency and voltage through PECs. For limited speed control (± 30% around ideal no-load speed) the variable rotor frequency supply method (through limited power PECs) is particularly suited for the scope, especially in high power drives.
- Stator frequency variation is followed along three methods of practical interest: V_1/f_1 method, constant rotor flux and constant stator flux methods.
- Only for constant rotor flux is the torque/speed curve linear (as for a PM DC brush motor) that is, ideal for electric drives control. This method is known as vector control.
- Split-phase capacitor induction motors are used in general below 500 W in single phase supply (home) applications.

8.22. PROBLEMS

8.1. Draw the complex root (eigenvalues) locus plot of a cage rotor induction motor with data as in example 8.2 for 8 different rotor speed values from zero to 2400 rpm, in stator coordinates ($\omega_b = 0$).

8.2. For the induction motor with resistances and inductances as in example 8.3, p = 1, $V_r^b = 0$, n = 900rpm, rotor flux $\lambda_r^b = 1$ Wb, torque level T_e = 40 Nm calculate: primary frequency ω_1, stator flux space-phasor amplitude in synchronous coordinates, stator voltage, stator current and power factor. Align the d axis along the rotor flux and draw the space-phasor diagram with the corresponding numbers on it (as in Figure 8.12).

8.3. An induction motor has the data ideal no-load (S = 0) phase current (rms) I_{on} = 5 A, p = 2, no-load losses p_0 = 200 W, stator phase voltage V = 120 V (rms); f_1 = 60 Hz; starting current per phase ($\omega_r = 0$, S = 1) $I_{start} = 15I_{on}$ and starting power factor $\cos\varphi_{1s} = 0.3$; $L_{ls} = L_{lr}$; $r_{start} = 3r_r$. Using the equivalent circuit of Figure 8.11 calculate: the stator and rotor resistances r_s, r_{start} and the leakage inductances L_{ls} and L_{lr}, the starting torque, core loss resistance r_m and core loss p_{iron}, and main inductance L_m. Observing that we have a deep bar (skin effect) rotor and the rotor resistance during normal operation is $r_r = 1.2r_s$, calculate all the electrical losses in the machine for S = 0.02.

8.4. For an induction motor with the data: $r_s = 0.2\ \Omega$, p = 2, $r_r = 0.2\ \Omega$, $L_{lr} = L_{ls} = 5\text{x}10^{-3}$ H, ($L_m = 0.1$ H), $f_1 = 60$ Hz, $V_L = 220$ V (rms) operating in regenerative braking at S = -0.02, calculate electromagnetic torque T_e and the electric power retrieved if the core and mechanical losses are neglected.

8.5. For the induction motor with the data (resistances and inductances) of problem 8.4, calculate the DC braking peak torque (for the DC connection of Figure 8.15b at $I_o = 4$ A), for $\omega_1 = 2\pi 10$ rad/s.

8.6. An induction motor works with a rotor flux level $\lambda_{r0} = 1$ Wb and has four poles (2p = 4) and the rotor resistance $r_r = 0.2\ \Omega$. For $\omega_1 = 2\pi 20$rad/s calculate and draw the torque/speed curve. For $\tau_r' = 0.01$s, S = 0.1, $K_s = 0.95$ determine the stator flux level λ_{so} and, neglecting the stator resistance, the stator voltage V_{s0} required.

8.7. An induction motor works at constant stator flux and variable frequency and has the data as in problem 8.6. Determine the critical slip frequency and $(S\omega_1)_k$ and the critical (breakdown) torque for $\lambda_{s0} = 1.06$ Wb and draw the torque/speed curve for $f_1 = 20$ Hz. For $f_1' = 60$ Hz, calculate the maximum flux level available for the same voltage as in the case of 20Hz, and determine again the breakdown torque available, and the corresponding electromagnetic power.

8.23. SELECTED REFERENCES

1. **K.P. Kovacs, I. Racz**, Transient regimes of AC machines, Springer Verlag 1995 (the original edition, in German, in 1959).
2. **P. Vas,** Vector control of AC machines, O.U.P., 1990.
3. **I. Boldea, S.A. Nasar,** Vector control of AC drives, Chapter 2, CRC Press, Florida, USA, 1992.
4. **D.W. Novotny, T.A. Lipo**, Vector control and dynamics of AC drives, Oxford University Press, 1996.
5. **R.H. Park**, "Two reaction theory of synchronous machines: generalized method of analysis", AIEE Trans.vol.48, 1929, pp.716-730.
6. **J. Holtz**, "On the spatial propagation of transient magnetic fields in AC machines", IEEE Trans.vol.IA-32, no. 4, 1996, pp.927-937.
7. **I. Boldea, S.A. Nasar**, "Unified treatement of core losses and saturation in orthogonal axis model of electric machines", Proc.IEE, vol.134, PartB, 1987, pp.355-363.
8. **I. Boldea, S.A.Nasar,** Induction machine handbook, CRC Press 2001.